ELSEVIER

Biochimica et Biophysica Acta 1369 (1998) 204–212

BIOCHIMICA ET BIOPHYSICA ACTA
BBA

Chronopotentiometric studies of electroporation of bilayer lipid membranes

Sławomir Kalinowski [a,*], Grażyna Ibron [b], Krzysztof Bryl [b], Zbigniew Figaszewski [a,1]

[a] *University of Warsaw, Białystok Branch, Institute of Chemistry, Al. J. Piłsudskiego 11 / 4, 15-443 Białystok, Poland*
[b] *University of Agriculture and Technology, Department of Physics and Biophysics, 10-957 Olsztyn-Kortowo, Poland*

Received 1 July 1997; accepted 10 September 1997

Abstract

The constant-intensity current chronopotentiometric measurements of egg yolk phosphatidylcholine bilayer membranes (BLM) are presented. It is demonstrated that a constant-intensity current flowing through the bilayer membranes generates the pores in their structures. For the current intensity from 0.1 to 2.0 nA, the generated pores open and close cyclically. The frequency of oscillations depends on the current intensity: the higher current intensity, the higher frequency of pore oscillations. It is suggested that the presented method may allow to create one pore in BLM and to observe its dynamical behaviour. Based on chronopotentiometric curves, a method of pore conductance calculations is presented. It is demonstrated that the value of obtained conductance can be applied for pore diameter estimation. The hypothetical application of constant-current method as a biotechnological tool for selective and controlled incorporation of molecules into microorganisms is discussed. © 1998 Elsevier Science B.V.

Keywords: Chronopotentiometry; Electroporation

1. Introduction

Electric modulation of biological membrane physical properties, electrical oscillations and excitations are natural processes of a cell [1–4]. Traditionally, external electric fields have been used as tools to probe these phenomena [5].

Recently, the application of external electric fields has gained increasing importance for manipulations in biological cells and tissue. In particular, the membrane electroporation methods were successfully used for loading exogenous molecules or ions into living cells [6], transdermal drug delivery [7], enzyme insertion into the membrane of blood organelles [8], transfer of genes, other nucleic acids and proteins into the interior of cells [9–12].

Despite the widespread use of the external electrical fields in biology, medicine and biotechnology [13–15], the underlying mechanism of the field-induced restructuring of the membrane is not yet satisfactorily understood [16,17]. However, this information is required to improve the present electroporation techniques for wide applications.

* Corresponding author. University of Agriculture and Technology, Department of Chemistry, 10-957 Olsztyn-Kortowo, Poland. Fax: (+48) 89 5273908; E-mail: kalinow@art.olsztyn.pl

[1] On leave from Faculty of Chemistry, Warsaw University, Pasteura 1, 02-093 Warsaw, Poland.

PII S0005-2736(97)00222-8

There are two major types of electroporation experiments: voltage clamp and charge pulse [5]. In both type of experiments, the mean lifetime of the membrane rapidly drops with increasing voltage, causing the experiments to become less effective. In particular, in the case of planar lipid bilayers (BLM) which are often used as a model system to investigate the electoporation, application of a steady potential in the order of few hundred mV, across a membrane, causes the membrane to break [18]. Therefore, only the action of very short electric pulses can be investigated with this method [19]. Hence, the fundamental problem is to eleborate a more effective method and a more stable system for electroporation investigations. In order to solve the second problem, it was demonstrated, for example, that treatment of BLM lipids by uranyl ions led to a considerable increase of the membrane electrical stability [20,21]. But this approach is not free of doubt that chemicals used may introduce additional, not existing in natural system, phenomena that must be additionally clarified [22]. The clue of solving first problem might be related to change the experimental conditions and to work in current-clamp conditions. It was suggested that, under current-clamp conditions, the membrane does not rupture because of the reduction of the transmembrane voltage, when the membrane conductance increases [19].

The following study was motivated from the foregoing account. The planar lipid membranes selected were not modified. Instead of voltage-clamp conditions, the electroporation phenomenon was studied under constant-intensity current (current-clamp) conditions. The chronopotentiometric ($U = f(t)$) characteristics of the membrane, registered under constant current intensity, demonstrate reversible conductance transitions to a higher conductance levels. The reversible conductance transition is interpreted as resulting from the generation of oscillating pores under constant-current conditions.

It is established that the frequency of oscillation may be regulated by intensity of current applied. The oscillating states might be maintained for a fairly long time. This suggests that the presented method might be applied for continuous observation of pore dynamical behaviour.

The advantage of constant current method is that these transitions cannot be observed under voltage-clamp conditions because the high-conductance state causes the membrane to break.

2. Materials and methods

2.1. Chemicals

Egg yolk phosphatidylcholine was purchased from Fluka (Buchs, Switzerland) and no further purification was performed. Analytical grade *n*-decane was purchased from POCH (Gliwice, Poland) and was additionally purified by distillation. Analytical-grade KCl was obtained from POCH (Gliwice, Poland) and was calcinated for 2 h at a temperature of 650°C for removing the organic impurities. De-ionized and reverse-osmotic treated water was distilled with a quartz still. The electrolytes were buffered with HEPES (Sigma, St. Louis, USA) to pH 7.0. The pH of the unbuffered electrolytes was ~ 6.3.

2.2. Measurements employing artificial membranes

Planar bilayer lipid membranes created by the Mueller–Rudin method were used [23]. The membranes were formed in a 1 mm diameter, round aperture in a hydrophobic partition between two Teflon compartments filled with 10 ml of 0.1 M KCl each.

The formation of the membranes was monitored both, visually and electrically. The orifice of the aperture with the membrane was photographed in transmitting light. The photographs were used for an estimation of the bilayer area.

Along with the visual inspection, electrical monitoring of the membrane formation was performed by measuring the capacitance. It was assumed that the membrane formation was complete when its capacitance was > 1.5 nF and the capacitance drift was < 10 pF/min.

The capacitance-to-period conversion method was used for capacitance measurements [24,25]. Voltammetric and chronopotentiometric measurements were performed using a four-electrode potentiostat-galvanostat described earlier [26]. The electrodes were Ag/AgCl with an average area of 0.5 cm^2. Experiments were performed at 25 ± 1°C. The data were processed and analysed with the computer program Excel (Microsoft).

3. Results

The chronopotentiometric characteristics of bilayer lipid membranes (BLM) under constant-current conditions were registered for several constant current intensities.

Fig. 1 shows typical chronopotentiometric curves registered with different constant-currents flowing through the bilayer lipid membrane: (a) – 0.1, (b) – 0.3, and (c) – 1.0 nA. The shape of these curves strongly depends on the current intensity. For low current intensity, the membrane voltage rises within a few seconds, reaching a constant value (Fig. 1, curve a).

Higher current intensity causes an increase in the membrane voltage, followed by its sudden decrease (Fig. 1, curve b). However, the membrane is not destroyed. By keeping current intensity constant, the voltage oscillations can be observed.

The typical irreversible breakdown curve characterising the destruction of membrane is shown on Fig. 1, curve c. A current intensity of 1.0 nA was too high for this membrane, which is demonstrated by the sudden disappearance of the membrane voltage – indicating destruction of the membrane.

Fig. 2 shows an example of chronopotentiometric curves registered sequentially for one membrane at three different constant current intensities: (a) – 0.2, (b) – 0.5 and (c) – 1.0 nA. The shape of these curves is very similar to the curve (b) in Fig. 1, although the measurements were performed on another membrane. Switching on the current caused a rapid membrane voltage increase. After reaching the value of 210 mV, the voltage drops sharply below the value of 100 mV. But it does not reach the starting value of 0 mV. Instead, potential oscillations ca. 100 mV are registered. The curves (a), (b) and (c) in Fig. 2 demonstrate the sequence of measurements: after registration of curve (a), the measurements were terminated for 30 s. Then, a second chronopotentiometric curve was registered at higher constant-intensity current (curve (b)). After the same time of termination, the third chronopotentiometric curve was registered (curve (c)). The starting increase of the membrane

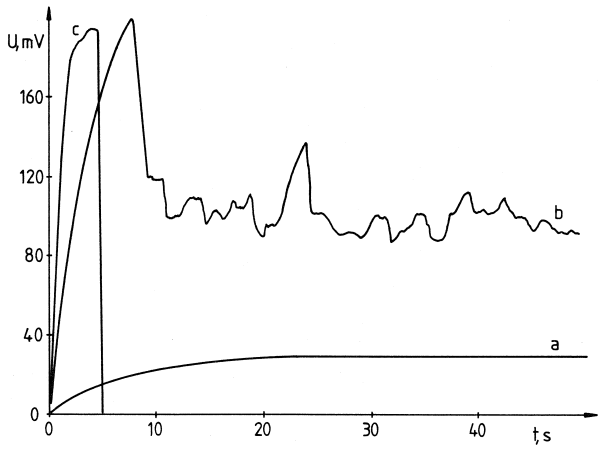

Fig. 1. Typical chronopotentiometric curves of bilayer lipid membranes registered for different constant intensity currents: (a) 0.1 nA, (b) 0.3 nA, (c) 1.0 nA. Forming solution: phosphatidylcholine in *n*-decane, 20 mg/ml. Electrolyte: 0.1 M KCl.

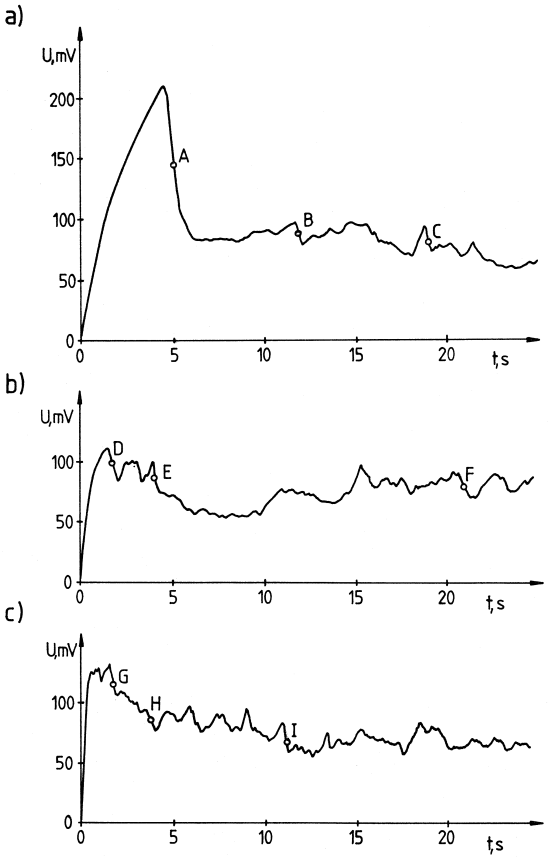

Fig. 2. Chronopotentiometric curves registered during reversible electric breakdown of bilayer lipid membrane. Current intensity: a) 0.2 nA, b) 0.5 nA, c) 1.0 nA. Forming solution: phosphatidylcholine in *n*-decane, 20 mg/ml. Electrolyte: 0.1 M KCl, 10 mM HEPES, pH 7.0. Points A-I were chosen for the pore conductance calculation.

voltages (for second, third, and other measurements) was lower than the voltage increase represented by the first chronopotentiometric curve. Also, voltage oscillations were observed around lower voltage values. It was possible to register several chronopotentiometric curves for one membrane. The same tendency was observed for all measurements. Points (A)–(I) will be described in Section 4.

Fig. 3 presents another set of chronopotentiometric curves registered for a membrane different from the one used for masurements presented in Fig. 2. The measurements were performed for constant current intensity of (a) – 0.2, (b) – 0.5 and (c) – 0.7 nA. Again clear potential oscillations can be observed.

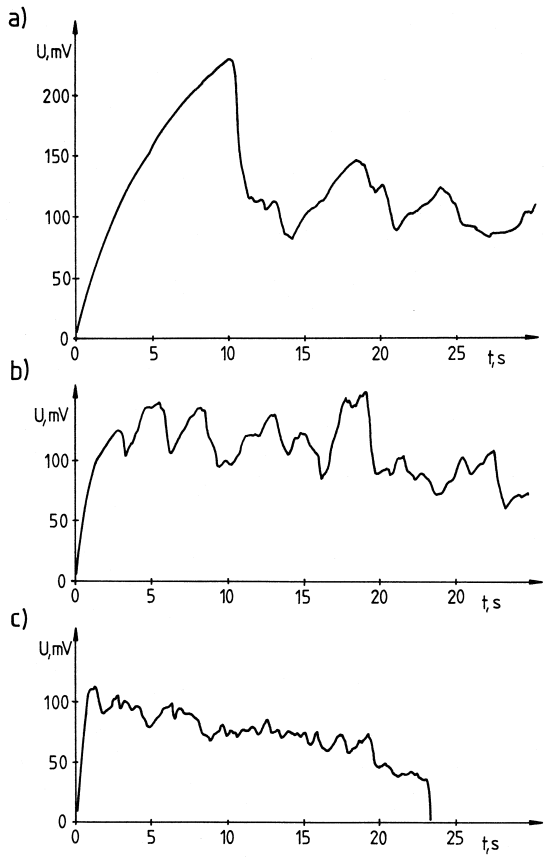

Fig. 3. Chronopotentiometric curves registered during reversible electric breakdown of bilayer lipid membrane. Current intensity: a) 0.2 nA, b) 0.5 nA, c) 0.7 nA. Forming solution: phosphatidylcholine in *n*-decane, 20 mg/ml. Electrolyte: 0.1 M KCl, 10 mM HEPES, pH 7.0.

For all the registered curves, a similar tendency can be distinguished: higher constant-intensity current causes an increase of frequency of oscillations and decrease of their amplitudes. The parameters of system used, namely membrane capacitance, current intensity, conductance and resolution of apparatus defined the upper limit for frequency measurements. So far, the highest frequency of 30 Hz has been registered. However, this fact does not exclude the possibility of higher membrane potential oscillations.

4. Discussion

The constant-intensity current flowing through the artificial bilayer lipid membranes causes an increase in the membrane potential (Fig. 1). The speed of changes in membrane potential depends on the intensity of the flowing current: higher the current intensity, the faster is the membrane potential increase. However, if the intensity of the current is too high, the membrane potential can suddenly drop to 0 mV – indicating the destruction of the membrane. The intensity of the current causing irreversible breakdown depends mainly upon materials for membrane preparation used.

In the case of moderate speed of potential changes, i.e. moderate constant-intensity current, it is possible to attain a state, where the membrane potential oscillations are observed in a chronopotentiometric curve (Fig. 1, curve b). The explanation of this phenomenon is based on changes in the electric properties of the membrane, induced by a constant current flowing through the membrane.

The constant-intensity current flowing through bilayer lipid membrane causes an increase in the membrane voltage within the first few seconds of registration. The membrane voltage increases to a value at which a defect structure is formed. The appearance of this structure causes a rapid increase of the membrane conductance and, as a result, a drop in the membrane voltage. On the other hand, decreasing membrane voltage influences the electrical field strength. If the field strength is lower than the critical field, which induces a breakdown potential, the defect structure cannot exist, and disappears. But this new membrane structure can guarantee the electrical

conditions in which the membrane voltage may increase again. The phenomenon of consecutive voltage decrease and increase about a certain voltage value is repeated in time, and is manifested as a chronopotentiometric curve oscillations (Fig. 1, curve b).

While transforming the oscillations of the electrical properties of bilayer membranes into their mechanical properties, it can be stated that under constant-intensity current conditions it is possible to generate an oscillating defect in bilayer membranes.

The voltage jumps, representing the creation of the defect, appear at voltage thresholds corresponding to the opening of pores in bilayer lipid membranes observed in voltammetric curves [26] or when the voltage pulses are applied for electroperforation [27]. This suggests that the oscillating defect structures generated by constant-intensity currents in our experiments have the same structures as classic electropores or are simply electropores. Therefore, we can qualitatively interpret the phenemenon as due to the electric-field-induced formation of pores. The voltage fluctuations are consistent with the notion that the pores have a characteristic relaxation time for closing when the potential is reduced [19,28].

Although the structure of pores has been suggested in drawings, their actual structure remains unknown. Because of the transient nature of the pores and the property of microscopy, such pores are not likely to be directly visualised. Instead, their structure must be inferred [29]. Here, we have shown that the registration of $U = f(t)$ under constant-current intensity conditions allows a simple estimation of pore parameters.

4.1. Estimation of the size of electropore generated by constant- intensity current

Fig. 2 presents an example of chronopotentiometric curves for one bilayer membrane, registered at different constant-intensity currents: (a) – 0.2, (b) – 0.5, and (c) – 1.0 nA. The membrane resistance was calculated from the voltametric curve registered before electroporation: $R_M = 1.5\,G\Omega$. The method of pore conductance calculation is presented in Appendix A. The results of calculations are summarised in Table 1. For the sake of checking the evolution of pore and reversibility of membrane structure, the calculations were performed at three independent points for each chronopotentiometric curve, registered under different constant-intensity current. Points A, B, C were chosen for the curve registered under current of 0.2 nA; points (D, E, F) and (G, H, I) under 0.5 and 1.0 nA, respectively.

The distribution of conductance for each set of points is rather small, suggesting that membrane structure oscillates with time around certain structures characteristic of (or defined by) current flowing through the membrane.

The average conductances are 3.6, 9.69 and 17.17 nS, calculated for chronopotentiometric curves

Table 1
Conductance and diameter of pores induced in bilayer lipid membranes under constant-current intensity conditions. The forming solution: phosphatidylcholine in *n*-decane, 20 mg/ml. Electrolyte solution: 0.1 M KCl, 10 mM HEPES, pH 7.0. The pore conductances are calculated for points marked on the Fig. 2

Point	Current intensity, i ([nA)	Voltage, U_M (V)	Slope, V_p (mV/s)	Slope, V (mV/s)	Pore conductance, G_p (nS)	Pore diameter, d (nm)
A	0.2	0.133	−140.1	42.7	3.63	5.01
B	0.2	0.088	−55.3	64.8	3.00	4.55
C	0.2	0.080	−87.7	69.6	4.17	5.37
D	0.5	0.102	−41.4	33.1	9.58	8.14
E	0.5	0.095	−56.3	37.3	11.6	8.94
F	0.5	0.080	−31.3	76.4	7.89	7.39
G	1.0	0.117	−116.1	90.4	18.0	11.2
H	1.0	0.086	−39.6	266.8	12.7	9.36
I	1.0	0.068	−150.7	309.9	20.8	12.0

registered under constant currents of 0.2, 0.5 and 1 nA, respectively. Surprisingly, this result demonstrates an almost linear relationship of pore conductance with constant current applied. This conductance change suggests that all of these points can be related to one oscillating electropore or to one type of appearing and disappearing electropores.

Although, it is difficult to obtain a real pore structure, we tried to calculate the size of pore basing on simplified assumptions. The following assumptions were made: the cylindrical shape of a pore was considered, the pores were filled with the same electrolyte as a bulk electrolyte, and the change of the temperature inside the pores, as a result of current flow, did not significantly change the pore conductance. The thickness of pores was assumed to be $d = 7$ nm. Although different pore shapes and, correspondingly, different pore energies can be considered, we use here the simplest possible shape, that of a cylindrical pore filled with electrolyte. This relatively simple approach is quite popular, because it leads to a reasonable quantitative description of several important phenomena [30]. The calculated pore parameters are presented in Table 1.

The effective surface area of pores calculated from the highest values of conductance were 0.226×10^{-16} m^2 ($i = 0.2$ nA), 0.627×10^{-16} m^2 ($i = 0.5$ nA), and 1.129×10^{-16} m^2 ($i = 1.0$ nA). Which, in turn, gave maximum effective pore diameters of 5.37, 8.94, and 12.0 nm, respectively (Table 1).

The estimation of the number of pores is very difficult (see, e.g. Refs. [30,31]). The estimations are usually based on a comparison between the calculated pore radii from experimental data with simplified models aiming at a description of electroporation phenomena. Benz at al. [32] estimated that the conductivity of 2.8 and 280 nS should correspond to the aqueous channel of 1 and 10 nm in diameter, respectively. In the transient aqueous-pore theories, in which the appearance of a heterogeneous pore population is fundamental, assuming a very simple, circular cylinder geometry used to represent a pore, the predicted mean pore radii are as follows [29]: 5–10 nm for square pulses, 1.5–10 nm for exponential pulses and 1–3 nm for bipolar square pulses. Similar (1–8 nm) pore diameters can be found in literature (see Refs. [33,34]). That is why it seems to us that the calculated diameter of ca. 5 nm can be interpreted as a mean diameter of one pore. Therefore, it is resonable to suggest that, under constant current conditions, we have observed a single pore, which is cyclically openning and closing. In presented method, the voltage increases slowly. The creation of the first pore causes a drastic decrease of membrane potential. In turn, this decreases the probability of next pore creation. Due to potential fluctuation, it is possible for a membrane to contain such a pore without rupturing. Such a pore can achieve a quasi-steady state for long periods.

Although we keep in mind the suggestion [29] that: ‘‘... theoretical models that involve only a single size pore will be incomplete and, therefore misleading,’’ it is reasonable to assume that presented method allows to generate one oscillating pore.

Three different pore diameters were obtained from experiments in which different constant currents were applied. The higher the current, the larger is the pore diameter. A clear increase in the pore diameter with increasing applied current can, in principle, be explained by:

1. the increased number of pores;
2. the increased mean radius of the pore; and
3. the nonlinear character of the resistance of small pores [31].

The third explanation is difficult to verify in our case, because it would be necessary to register pore conductivity during its oscillations. According to the already presented hypothetical mechanism of pore creation, the increased number of pores seems to be unlikely. Finally, it seems quite possible that high currents, passing through the membrane close to breakdown areas, cause structural changes in the membrane. This is reflected by the increased mean radius of the pore. It is important to emphasise that the generated quasi-states are highly resistant to destruction, and the membrane is not ruptured. For the highest current intensities used, the pore diameter was larger than the assumed membrane thickness, but the lifetime of this state was still long.

Two sets of three model curves were chosen (Figs. 2 and 3) to present the described phenomena and to present the method of pore conductivity and diameter calculations. The main task of our work was to present the method of one pore generation and the method of analysing such dynamic behaviour of the pore. The points, at which curve $U(t)$ is the steepest,

were chosen for pore conductivity and diameter calculations. Values, calculated at these points, represent the highest value of pore conductivity and the largest pore diameter. The analysis of many curves do not indicate significant differences in the value of maximal conductivity.

4.2. Gradual closing of an electropore generated by a constant-intensity current

A number of studies have shown that molecular transport through an electropore can occur within seconds or hours after a pulse [33,35–37]. Complete resealing of electropores requires a long period of time, depending on the lipids and environment conditions used for bilayer membrane creation [38].

In constant-intensity current conditions, it is possible to generate a state where subsequent chronopotentiometric measurements added states in which a pore is increasingly opened or the membrane is locally more and more deformed. As it can be seen from Figs. 2 and 3, once the constant current was turned off, the pore began to shrink. However, this electropore was never completely resealed. The consecutive switching on and off of the constant-current flow leaves the former pore in a less closed state or introduces a greater membrane deformation. The membrane does not return to the state of continuous structure. The permanent deformation is created in the place where the first pore appears. Hence, lower membrane potential is required for pore opening. In our experiments, we achieved a shift of oscillation level from hundreds to tens of millivolts. A comparison of the final conductance and geometric parameters of pores, generated in consecutive chronopotentiometric measurements, suggests that pores behave in a similar way under external stress (e.g. constant current). It reaches the fully open state similar to that reached by first pores. Only, a lower membrane voltage is required to induce pore oscillation.

One can speculate about the cellular mechanism for regulating the efficiency of membrane permeability for molecules, important for living processes. Instead of the creation of a large number of pores (channels), the repetition of constant-current flow through a membrane can guarantee the existence of a sufficiently permeable membrane structure. An additional feature of the described phenomenon may be utilised by living organisms: cells can drastically lower the threshold of membrane potential required for generating a fully open pore state. The frequency of repetition might be regulated by the living organism itself.

The oscillating states might be mantained for a fairly long time in a model system. It is demonstrated that the frequency of oscillation may be regulated by intensity of the current applied. This may suggests technical applications for increasing (or decreasing) the efficiency of molecule incorporation into the cell. In the case of pulse method or voltage-clamp conditions, the elementary process, once started, cannot be changed.

The constant-current method works well in BLM model systems. The question arises whether this method could be applied as a biotechnological tool for selective (pore diameter) and controlled (frequency of oscillations) incorporation of molecules into a microorganism. To answer this question, the experiments with cells and whole microorganism should be performed.

Appendix A. Estimation of the electric parameters of electropores generated by a constant-intensity current

Fig. 4(a) shows an equivalent electric circuit for the bilayer lipid membrane. The bilayer lipid membrane can be considered as a parallel-plate capacitor

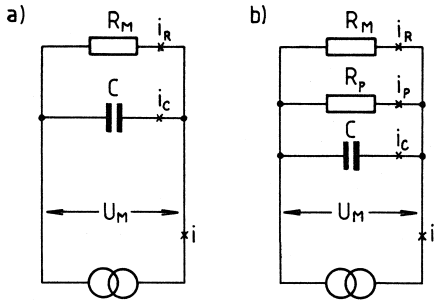

Fig. 4. Equivalent electrical circuits of the bilayer lipid membrane: a) the membrane without pores, b) the membrane with pores. R_M – membrane resistance, R_P – resistance of pores, C – membrane capacitance, i_P – current flowing through pores, i_R – membrane resistance current, i_C – membrane capacitance current, i – total current flowing through the electrodes and the membrane.

(C_M), in parallel with its resistance (R_M). The current (i) flowing through electrodes creates a membrane voltage (U_M) which reaches a constant value in a few seconds (Fig. 1, curve (a)).

According to Kirchhoff's law, the current (i) is the sum of currents flowing through resistance (i_R) and that flowing through a capacitor (i_C):

$$i = i_C + i_R \tag{A.1}$$

The time for reaching the membrane voltage U_M may be different for different membranes, because the rate of membrane voltage changes depends on the membrane capacitance and the capacitance current i_C.

Let us introduce the factor V, which represents a slope at the selected point of the chronopotentiometric curve dU/dt:

$$V \equiv \frac{dU}{dt} = \frac{i_C}{C} \tag{A.2}$$

Considering Eq. (A.1), the factor V can be calculated as:

$$V = \frac{i - i_R}{C} \tag{A.3}$$

V describes the rising parts of curves (a)–(c), presented in Fig. 1, irrespective of further changes in membrane structure. But perforation of the bilayer planar lipid membrane causes a decrease in its resistance. The kinetics of voltage changes for the perforated membrane (V_p) may be different from that for a membrane without pores (V) (Fig. 5).

Fig. 4(b) shows an equivalent electrical circuit for bilayer lipid membrane with pores. The resistance R_P denotes resistance of pores created. If i_p defines the current flowing through the pores, then Eq. (A.1) must be supplemented with this current and, consequently, the slope of the curve for perforated membrane V_p can be described by:

$$V_p = \frac{i - i_R - i_p}{C} \tag{A.4}$$

It is known that bilayer lipid membrane capacitance and resistance current are dependent on membrane voltage [39]. This fact makes the measurements more complicated. However, making calculations for the same value of membrane voltage U_M, Eqs. (A.3) and (A.4) gives equal values of membrane capacitance C (Fig. 5).

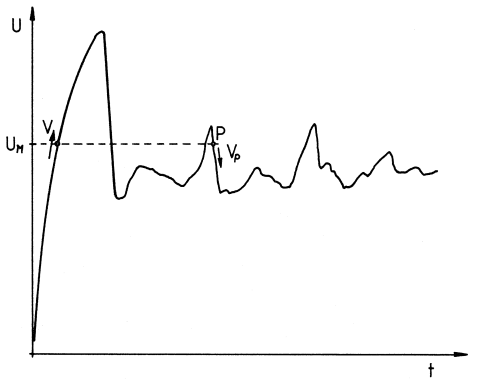

Fig. 5. Hypothetical chronopotentiometric curve with marked parameters used for calculation of pore conductance in chosen point P. Slope V, V_p and membrane potential (U_M) are described in text.

Hence, the current flowing through pores is given by:

$$i_p = (i - i_R)\left(1 - \frac{V_p}{V}\right) \tag{A.5}$$

Pore conductance, G_P, is a function of the membrane voltage U_M and the current flowing through the pores:

$$G_p = \frac{i_P}{U_p} \tag{A.6}$$

Considering Eq. (A.5), and the fact that the resistance of bilayer lipid membrane without pores (R_M) is independent of the membrane voltage U_M, i.e. R_M obeys the Ohm's law, $U_M = i_R \times R_M$, pore conductance can be calculated from:

$$G_p = \left(\frac{i}{U_M} - \frac{1}{R_M}\right)\left(1 - \frac{V_p}{V}\right) \tag{A.7}$$

Bilayer lipid membrane usually has very high resistance, and therefore, the factor $1/R_M$ can be neglected in Eq. (A.7). In this case, the pore conductance can easily be calculated. Otherwise, R_M must be estimated. Generally, membrane resistance is not reproducible and can vary greatly from membrane to membrane despite the same lipids being used for membrane preparation. Hence, R_M for each membrane used for experiments should be estimated from independent measurements.

Membrane capacitance measurements for the same membrane voltage may be slightly different for growing and decaying directions of voltage change. Hence, the factors V and V_P can differ from real values only due to the different direction of the voltage change. We have estimated this error. Because, under our experimental conditions, the error was $< 5\%$, we used Eq. (A.7) for pore conductance calculations without any correction.

References

[1] R.B. Gennis, Biomembranes. Molecular Structure and Function. Springer-Verlag, New York, 1989.
[2] M. Ikematsu, M. Iseki, Y. Sugiyama, A. Mizukami, Bioelectrochem. Bioenerg. 36 (1995) 61–65.
[3] K. Urabe, H. Sakaguchi, Biophys. Chem. 59 (1996) 33–41.
[4] Ch.D. McCallum, R.M. Epand, Biochemistry 34 (1995) 1815–1824.
[5] D.C. Chang, B.M. Chassy, J.A. Saunders, A.E. Sowers (Eds.), Guide to Electroporation and Electrofusion, Academic Press, New York, 1992.
[6] S. Sixou, J. Teissie, Bioelectrochem. Bioenerg. 31 (1993) 237–257.
[7] S. Orlowski, L.M. Mir, Biochim. Biophys. Acta 1154 (1993) 51–63.
[8] U. Zimmermann, F. Riekmann, G. Pilwat, Biochim. Biophys. Acta. 436 (1976) 460–474.
[9] V.A. Klenchin, S.I. Sukharev, S.M. Serov, L.V. Chernomordik, Y.A. Chizmadzhev, Biophys. J. 60 (1991) 804–811.
[10] E. Neumann, E. Werner, A. Sprafke, K. Kruger, (1992) in: B.R. Jennings, S.P. Stoylov, (eds.), Colloid and Molecular Electro-Optics, IOP Publishing, Bristol. pp. 197-206.
[11] E. Neumann, A.E. Sowers, C.A. Jordan, Electroporation and Electrofusion in Cell Biology, Plenum Press, New York, 1989.
[12] J.C. Weaver, J. Cell. Biochem. 51 (1993) 426–435.
[13] G.V. Gass, L.V. Chernomordik, Biochim. Biophys. Acta 1023 (1990) 1–11.
[14] U. Zimmermann, G. Neil, Electromanipulation of Cells, CRC Press, 1995.
[15] U. Zimmermann, P. Gessner, M. Wander, S.K.H. Fuong, in: C. Borrebueck, and I. Hagen, (eds.), Electromanipulation in Hybridoma Technology, Stockton Press, NY, 1989, pp. 1-30.
[16] C. Wilhelm, M. Winterhalter, U. Zimmermann, R. Benz, Biophys. J. 64 (1993) 121–128.
[17] J.C. Weaver, Yu.A. Chizmadzhev, Bioelectrochem. Bioenerg. 41 (1996) 135–160.
[18] A. Barnett, J.C. Weaver, Bioelectrochem. Bioenerg. 25 (1991) 163–182.
[19] I. Genco, A. Gliozzi, A. Relini, M. Robello, E. Scalas, Biochim. Biophys. Acta 1149 (1993) 10–18.
[20] I.G. Abidor, L.V. Chernomordik, S.I. Sukharev, Yu.A. Chizmadzhev, Bioelectrochem. Bioenerg. 9 (1982) 141–148.
[21] L.V. Chernomordik, S.I. Sukharev, I.G. Abidor, Yu.A. Chizmadzhev, Bioelectrochem. Bioenerg. 9 (1982) 149–155.
[22] S.I. Sukharev, L.V. Chernomordik, I.G. Abidor, Yu.A. Chizmadzhev, Bioelectrochem. Bioenerg. 9 (1982) 133–140.
[23] P. Mueller, D.O. Rudin, H.T. Tien, W.C. Wescott, J. Phys. Chem. 67 (1963) 534–535.
[24] S. Kalinowski, Z. Figaszewski, Biochim. Biophys. Acta. 1112 (1992) 57–66.
[25] S. Kalinowski, Z. Figaszewski, Meas. Sci. Technol. 6 (1995) 1043–1049.
[26] S. Kalinowski, Z. Figaszewski, Meas. Sci. Technol. 6 (1995) 1050–1055.
[27] T.Y. Tsong, Biophys. J. 60 (1991) 297–306.
[28] R. Benz, U. Zimmermann, Biochim. Biophys. Acta 640 (1981) 169–178.
[29] S.A. Freeman, M.A. Wang, J.C. Weaver, Biophys. J. 67 (1994) 42–56.
[30] K.T. Powell, J.C. Weaver, Bioelectrochem. Bioenerg. 15 (1986) 211–227.
[31] L.V. Chernomordik, S.I. Sukharev, I.G. Abidor, Yu.A. Chizmadzhev, Biochim. Biophys. Acta 736 (1983) 203–213.
[32] R. Benz, F. Beckers, U. Zimmermann, J. Membrane Biol. 48 (1979) 181–204.
[33] M.R. Prausnitz, J.D. Corbett, J.A. Gimm, D.E. Golan, R. Langer, J.C. Weaver, Biophys. J. 68 (1995) 1864–1870.
[34] S. Kakorin, S.P. Stylov, E. Neumann, Biophys. Chem. 58 (1996) 109–116.
[35] H. Lambert, R. Pankow, J. Gauthier, R. Hancock, Biochem. Cell Biol. 68 (1990) 729–734.
[36] M.P. Rols, J. Teissie, Biophys. J. 58 (1990) 1089–1098.
[37] R.C. Lee, L.P. River, F. Pan, L. Ji, R.L. Wollmann, Proc. Natl. Acad. Sci. USA. 89 (1992) 4524–4528.
[38] T.Y. Tsong, Bioelectrochem. Bioenerg. 24 (1990) 271–295.
[39] R. Benz, O. Fröhlich, P. Läuger, M. Montal, Biochim. Biophys. Acta 394 (1975) 323–334.